CHAPTER 5 «CONTROL OF SHARPLY FOCUSED LASER BEAMS»

DOI: https://doi.org/10.30525/978-9934-26-461-0-5

THz electromagnetic radiation has a wide range of applications in high-speed communications, environmental monitoring, quality control of medicines and food, biology, and medical diagnostics. Despite of significant progress in the field of lasing and detecting of THz radiation, the appropriate research still remains one of the most rapidly developing area of contemporary applied physics.

A significant number of works in the field is devoted to development of lenses and diffraction gratings in the THz range. However, the extensive application of coherent THz radiation requires for creating the components with wider functional capabilities. Applications such as terahertz imaging (including extended objects), laser ablation, optical discharge generation, and others require focusing of terahertz radiation, often focusing with increased depth of focus. Accordingly, research on changing the focal region parameters is very relevant today.

In this chapter, we theoretically and experimentally study the possibility of controlling the parameters of the focal region formed by sharply focused laser beams from a THz laser based on a hollow circular dielectric waveguide.

5.1. THEORETICAL RELATIONS AND EXPERIMENTAL SETUP

Let us set the radiation in the initial plane as linearly polarized EH_{11} and azimuthally polarized TE_{01} modes. The normalized electric components E_r and E_ϕ of the given modes on the output mirror of the resonator in the cylindrical coordinate system are described in Chapter 3 (equations 4.2, 4.4).

Using the vector Rayleigh-Sommerfeld theory [142] in the nonparaxial approximation and the expressions of the field components of the EH_{11} and TE_{01} modes on the output mirror of the resonator, we find the field components of these modes in free space at the distance z_1 (Figure 5.1). For controlling the parameters of the focal region, we placed absorbing

masks on the lens. Multiplying the obtained expressions by the function of the phase correction of the lens, taking into account the dimensions of the absorbing masks and again applying the Rayleigh-Sommerfeld integrals to them, we find the components of the field of these modes in the focal region of the lens.

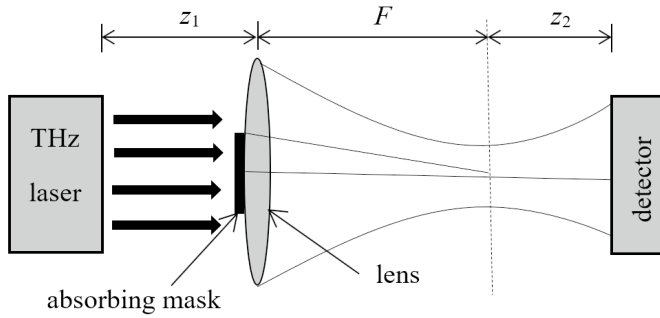

Figure 5.1. Theoretical model of control of sharply focused laser beams

The field components for the azimuthally polarized TE_{01} mode in the focal region of the lens, taking into account absorbing masks, have the form:

$$\begin{cases} E_r\left(\rho_2,\theta_2,F+z_2\right)=0, \\ E_\phi\left(\rho_2,\theta_2,F+z_2\right)=-\dfrac{k^2 z_1(F+z_2)}{\xi_2^{\,2}}\exp(ik\xi_2)A_{01}\displaystyle\int_{a_3}^{a_2}\frac{\exp(ik\xi_1)}{\xi_1^{\,2}}\int_0^{a_1}J_1\left(\chi_{01}\frac{r}{a_1}\right)\times \\ \qquad\times J_1(\gamma_1 r)\exp\left(\frac{ikr^2}{2\xi_1}\right)rdrJ_1(\gamma_2\rho_1)\exp\left(\frac{ik\rho_1^{\,2}}{2\xi_2}\right)Ph(\rho_1)\rho_1 d\rho_1, \\ E_z\left(\rho_2,\theta_2,F+z_2\right)=0. \end{cases} \tag{5.1}$$

where $k=2\pi/\lambda$ is the wavenumber, λ is the wavelength; z_2 is the distance from the focal plane of the lens to the receiver; ρ_1,θ_1,z_1 are the cylindrical coordinates in the lens plane; $\xi_1=\sqrt{z_1^{\,2}+\rho_1^{\,2}}$; $\gamma_1=k\rho_1/\xi_1$; ρ_2,θ_2,z_2 are the cylindrical coordinates in the observation plane behind the lens; $\xi_2=\sqrt{(F+z_2)^2+\rho_2^{\,2}}$; $\gamma_2=k\rho_2/\xi_2$, a_1 is the radius of waveguide;

a_2 is the lens radius; a_3 is the absorbing mask radius; $Ph(\rho_1) = \exp\left(-i\pi\rho_1^2 / \lambda F\right)$ is the lens phase correction function, F is the focal length of the lens.

The field components for the azimuthally polarized EH_{11} mode in the focal region of the lens, taking into account absorbing masks, have the form:

$$
\begin{cases}
E_r(\rho_2,\theta_2,F+z_2)=\dfrac{k^2 z_1(F+z_2)}{\xi_2^{\,2}}\exp(ik\xi_2)\sin(\theta_2)C_{11}\displaystyle\int_{a_3}^{a_2}\frac{\exp(ik\xi_1)}{\xi_1^{\,2}}\times \\
\times\displaystyle\int_0^{a_1} J_0\left(\chi_{01}\frac{r}{a_1}\right)J_0(\gamma_1 r)\exp\left(\frac{ikr^2}{2\xi_1}\right)rdrJ_0(\gamma_2\rho_1)\exp\left(\frac{ik\rho_1^{\,2}}{2\xi_2}\right)Ph(\rho_1)\rho_1 d\rho_1, \\
E_\phi(\rho_2,\theta_2,F+z_2)=\dfrac{k^2 z_1(F+z_2)}{\xi_2^{\,2}}\exp(ik\xi_2)\cos(\theta_2)C_{11}\displaystyle\int_{a_3}^{a_2}\frac{\exp(ik\xi_1)}{\xi_1^{\,2}}\times \\
\times\displaystyle\int_0^{a_1} J_0\left(\chi_{01}\frac{r}{a_1}\right)J_0(\gamma_1 r)\exp\left(\frac{ikr^2}{2\xi_1}\right)rdrJ_0(\gamma_2\rho_1)\exp\left(\frac{ik\rho_1^{\,2}}{2\xi_2}\right)Ph(\rho_1)\rho_1 d\rho_1, \quad (5.2) \\
E_z(\rho_2,\theta_2,F+z_2)=\dfrac{ik^2 z_1}{\xi_2^{\,2}}\exp(ik\xi_2)\sin(\theta_2)C_{11}\displaystyle\int_{a_3}^{a_2}\frac{\exp(ik\xi_1)}{\xi_1^{\,2}}\int_0^{a_1} J_0\left(\chi_{01}\frac{}{a_1}\right)\times \\
\times J_0(\gamma_1 r)\exp\left(\frac{ikr^2}{2\xi_1}\right)rdr\left[i\rho_1 J_1(\gamma_2\rho_1)+\right. \\
\left.+\rho_2 J_1(\gamma_2\rho_1)\right]\exp\left(\frac{ik\rho_1^{\,2}}{2\xi_2}\right)Ph(\rho_1)\rho_1 d\rho_1,
\end{cases}
$$

The scheme of the experimental setup is chosen similarly to the theoretical model, which is shown in Figure 5.1. The focusing system was represented by a short-focus lens with a numerical aperture of $NA = 0.68$, the central area of which was covered by absorbing masks of different diameters. The parameters of the focal region of the focused beam were determined using a pyroelectric point detector with a spatial resolution of 0.2 mm, which moved in three planes.

5.2. COMPARISON OF THEORETICAL AND EXPERIMENTAL RESULTS

Using the equation (5.1) and (5.2) we have evaluated the intensity distribution of sharply focused laser beams near the focus. The wavelength

of the radiation under study was 0.4326 mm (line of generation of a THz laser with optical pumping on the HCOOH molecule). The radius of the waveguide is chosen to be a_1 = 17.5 mm, the lens radius is a_2 = 25 mm, the radius of the absorbing masks varied in the range a_3 = 0 ÷ 17.5 mm. The focal length of the lens F = 36.4 mm, made of crystalline quartz, was chosen according to the condition of sharp focusing NA > 0.6. The distance z_1 was chosen 700 mm for complete beam interception. Let us estimate the influence of the parameter δ ($\delta = a_3/a_2$) on the distribution of the total field intensity ($I = |E_r|^2 + |E_\phi|^2 + |E_z|^2$) and on the diameter of the focused beams.

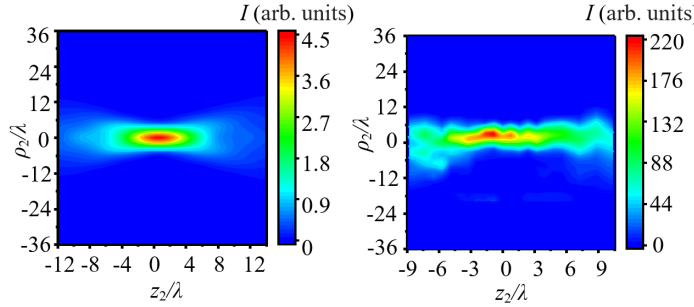

a) b)

Figure 5.2. Theoretical (a) and experimental (b) distributions of the total field intensity of EH_{11} mode in the focal region of the lens at δ = 0

The theoretical and experimental distributions of the total field intensity of linearly polarized EH_{11} mode of the dielectric resonator in the focal region without an absorbing mask (δ = 0) are shown in Figure 5.2. As can observe from the figure, the total field intensity has a maximum at the center of the focal spot. In the absence of an absorbing mask, the beam diameter of the mode at the focus (FWHM) was found to be equal 1.12 λ as per the calculations and 1.42 λ as per the experiment. At the same time, the depth of focus ℓ_z of the mode was found to be equal 1.20 λ in the calculations and 2.30 λ in the experiment. We will notice that ℓ_z defined in the study by the limit of increase of the beam diameter for 10 % of its minimum value.

By varying the parameter δ, it is experimentally shown that the maximum focus depth is achieved at δ = 0.6. The theoretical and experimental

distributions of the total field intensity for the linearly polarized EH_{11} mode in the focal region at δ = 0.6 are depicted in Figure 5.3. As can observe from the figure, the total intensity of the mode field at the center of the focal spot also has a maximum while the shape of the field distribution changes significantly.

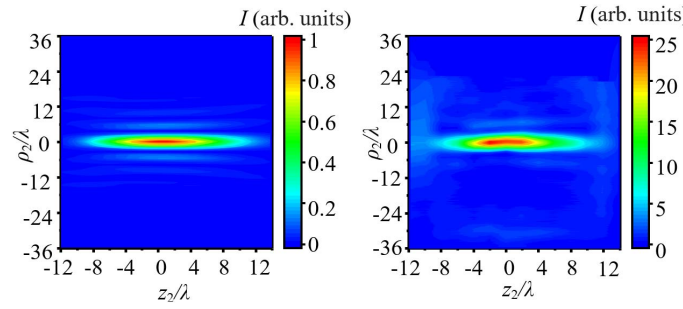

Figure 5.3. Theoretical (a) and experimental (b) distributions of the total field intensity of EH_{11} mode in the focal region at δ = 0.6

The beam diameter of the sharply focused EH_{11} mode at δ = 0.6 was found to be equal 0.76 λ in the calculations, and 1.00 λ in the experiment. The depth of focus of this mode in the calculations was found to be equal 19.00 λ, which is fully confirmed by the experimental results (ℓ_z = 19.60 λ). The theoretical and experimental de pendences of the beam diameter of sharply focused EH_{11} mode in the focal region on the distance z_2 at $\delta = 0$ and $\delta = 0.6$ are depicted in Figure 5.4.

The theoretical and experimental distributions of the total field intensity of azimuthally polarized TE_{01} mode of the dielectric waveguide resonator in the focal region at $\delta = 0$ are depicted in Figure 5.5.

As can observe from the figure, the distribution of the field intensity of this mode in the transverse plane of the beam has an annular shape. Moreover, in the absence of an absorbing mask, the beam diameter of the TE_{01} mode at the focus was found to be equal FWHM = 2.10 λ in the calculations, and FWHM = 3.20 λ in the experiment. The appropriate depth of focus was found to be equal 1.61 λ in the calculations, 1.40 λ in the experiment.

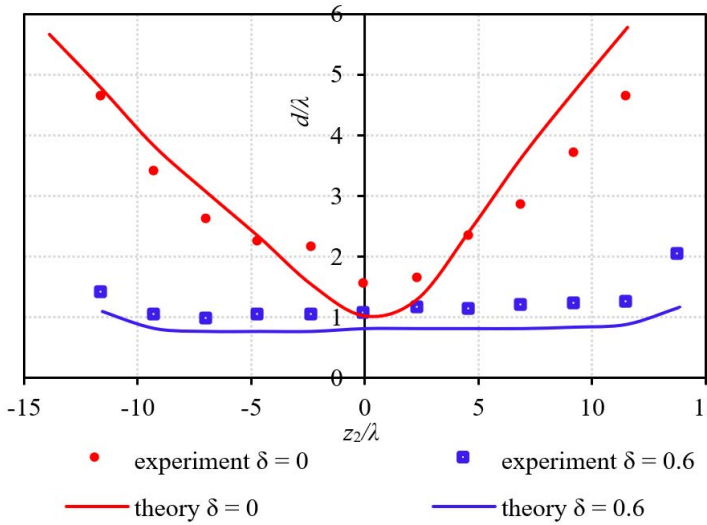

Figure 5.4. Theoretical and experimental dependences of the beam diameter of sharply focused EH_{11} mode on the distance z_2 at δ = 0 and δ = 0.6

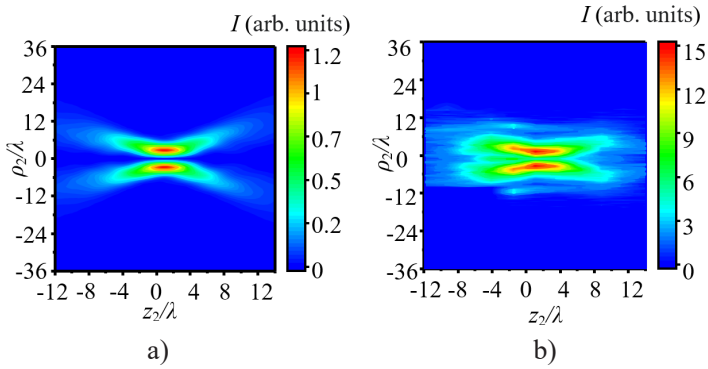

a) b)

Figure 5.5. Theoretical (a) and experimental (b) distributions of the total field intensity of TE_{01} mode in the focal region of the lens at δ = 0

For the sharply focused TE_{01} mode, the maximum focus depth and minimum beam diameter were achieved at $\delta = 0.45$. The appropriate distributions of the total field intensity of this mode in the focal region are depicted in Figure 5.6. The total field intensity of the TE_{01} mode at the focal spot remains ring-shaped.

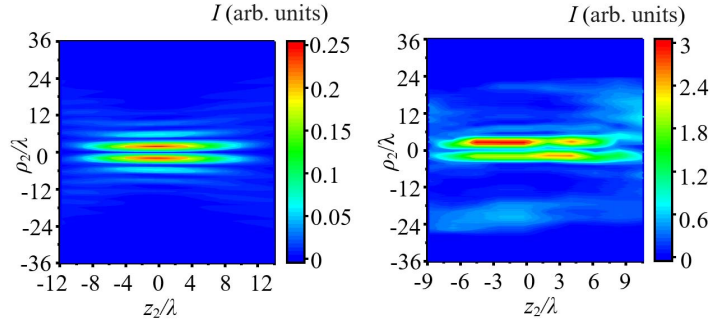

Figure 5.6. Theoretical (a) and experimental (b) distributions of the total field intensity of TE_{01} mode in the focal region at $\delta = 0.45$

However, the beam diameter and focus depth change significantly as per the case of EH_{11} mode. The beam diameter of TE_{01} mode at the focus was found to be equal FWHM = 1.70 λ in the theoretical calculations, and FWHM = 2.20 λ in the experiment. The depth of focus of the sharply focused mode at $\delta = 0.45$ was found to be equal 11.50 λ in the calculations, and 11.90 λ in the experiment (Figure 5.7).

Calculated and experimental transverse and longitudinal dimensions of focal spots for EH_{11} and TE_{01} modes when they are sharply focused with different parameters of the absorbing mask are given in Table 5.1. The laser radiation power in the absence of an absorbing mask on the focusing element for the EH_{11} mode was 4.3 mW, while in the case of using an absorbing mask it was 2.2 mW. Laser radiation power in the absence of an absorbing mask on the focusing element for TE_{01} mode was 2.2 mW, while in the case of using an absorbing mask – 1.4 mW.

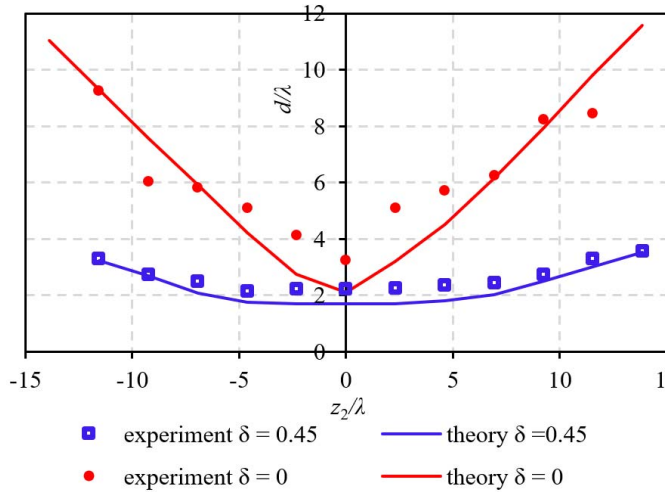

Figure 5.7. Theoretical and experimental dependences of the beam diameter of sharply focused TE_{01} mode on the distance z_2 at δ = 0 and δ = 0.45

Table 5.1

Focused beams parameters

Mode types	δ	Parameter	Theory	Experiment
EH_{11}	0	FWHM	1.12 λ	1.42 λ
		ℓ_z	1.20 λ	2.3 λ
	0.6	FWHM	0.76 λ	1.00 λ
		ℓ_z	19.00 λ\	19.60 λ
TE_{01}	0	FWHM	2.10 λ	3.20 λ
		ℓ_z	1.61 λ	1.40 λ
	0.45	FWHM	1.70 λ	2.20 λ
		ℓ_z	11.50 λ	11.90 λ